Potential dependent reorientation controlling activity of a molecular electrocatalyst

Adrian M. Gardner,[a,b] Gaia Neri,[a†] Bhavin Siritanaratkul,[a] Hansaem Jang,[a] Khezar Saeed,[a‡] Paul Donaldson[c] and Alexander J. Cowan[a*]

Addresses

[a] Department of Chemistry and Stephenson Institute for Renewable Energy, University of Liverpool, Liverpool, L69 7ZD, UK, acowan@liverpool.ac.uk

[b] Early Career Laser Laboratory, University of Liverpool, Liverpool, L69 3BX UK

[c] Central Laser Facility, STFC Rutherford Appleton Laboratory, Harwell, Didcot, Oxfordshire, OX11 0QX, UK

[†] Current address – Johnson Matthey, Sonning Common, Reading, RG4 9NH, UK

[‡] Current address - Department of Chemistry, Aarhus University, Langelandsgade 140, 8000, Aarhus, Denmark

Abstract: The activity of molecular electrocatalysts depends on the interplay of electrolyte composition near the electrode surface, the composition and morphology of the electrode surface, and the electric field at the electrode-electrolyte interface. This interplay is challenging to study and often overlooked when assessing molecular catalysts activity. Here we use surface specific vibrational sum frequency generation (VSFG) spectroscopy to study the solvent and potential dependent activation of $Mo(bpy)(CO)_4$, a CO_2 reduction catalyst, at a polycrystalline Au electrode. We find that the parent complex undergoes potential dependent reorientation at the electrode surface when a small amount of N-Methyl-2-pyrrolidone (NMP) is present. This pre-activates the complex, resulting in greater yields, at less negative potentials, of the active electrocatalyst for CO_2 reduction.

Main text: There is interest in developing new transition metal electrocatalysts for a range of applications relating to devices for fuel generation/consumption and energy storage. An advantage of molecular electrocatalysts is that they are synthetically tuneable, and in contrast to the more complex enzymatic centres from which inspiration is often drawn, their simplicity in-principle allows for evaluation of molecular structure - function relationships.[1,2,3] In addition to the role of the catalyst's structure on activity, important, but often overlooked, is how the molecular catalyst interacts with the electrode surface and the impact of the potential dependent composition of the electrolyte (solvent, supporting electrolyte) near to the electrode surface. Interfacial electric field effects and the subsequent impact of double layer structure on heterogeneous catalysts/metal electrodes are widely discussed to rationalise the behaviour of cation induced activity changes for example during CO_2 reduction.[4,5,6] However direct measurement of potential/field and solvent induced rearrangements of molecular electrocatalysts is rarer, despite it being reasonable to assume that there is impact on activity.[7,8,9]

Past studies by Hartl and colleagues have shown that the activity of the CO_2 reduction electrocatalyst $Mo(bpy)(CO)_4$ has a strong dependence on the nature of the electrode material and solvent.[2,10] The active catalytic species that binds CO_2 is $Mo(bpy)(CO)_3^{2-}$ (figure 1a).[10] Using VSFG spectroscopy, we have previously shown that when CH_3CN is the solvent a small population of this species is formed specifically on Au surfaces at potentials positive of those anticipated from the diffusion controlled redox potential,[11] explaining the improved catalytic activity at Au. The solvent dependent behaviour of this catalyst is not yet understood. Specifically NMP (NMP = N-Methyl-2-pyrrolidone) is known to enhance catalytic activity.[10]

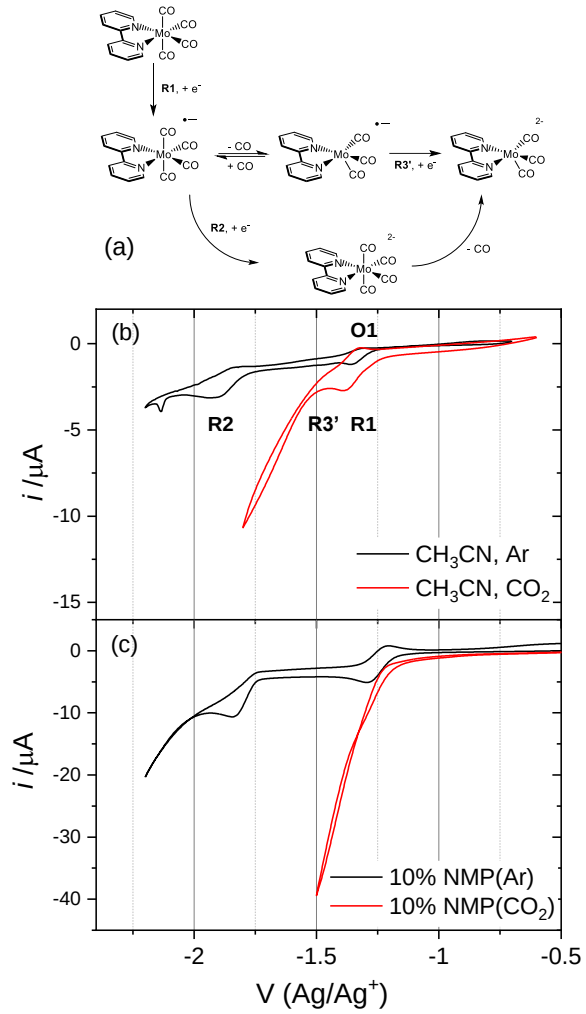

Figure 1. *CV's (20 mV s^{-1}) of $Mo(bpy)(CO)_4$ (1 mM) in CH_3CN (b) and CH_3CN with 10% (vol.) NMP (c) both with 0.1 M $TBAPF_6$ at Au electrode under Ar (black) and CO_2 (red). (a) Mechanism of formation of the active catalyst, $Mo(bpy)(CO)_3^{2-}$ in CH_3CN where a small population of $Mo(bpy)(CO)_4^-$ undergoes CO loss on Au and facile reduction (R3') to form $Mo(bpy)(CO)_3^{2-}$.*

Cyclic voltammograms (CVs) of $Mo(bpy)(CO)_4$ at a Au electrode in CH_3CN and CH_3CN with 10% (vol.) NMP are shown in Figure 1(b,c). $Mo(bpy)(CO)_4$ gives rise to a catalytic current for CO_2 reduction in both solvents but the onset is at more positive potentials and the magnitude of the catalytic current is greater when 10% NMP is added to the solution. Neat NMP has previously been shown to enhance the CO_2 reduction current.[10] The observation that even 10% NMP in CH_3CN can replicate this enhancement means it is not a result of the bulk solvent properties of NMP, and is instead proposed to be due to the way that NMP can interact with the electrocatalyst and/or the electrode surface.

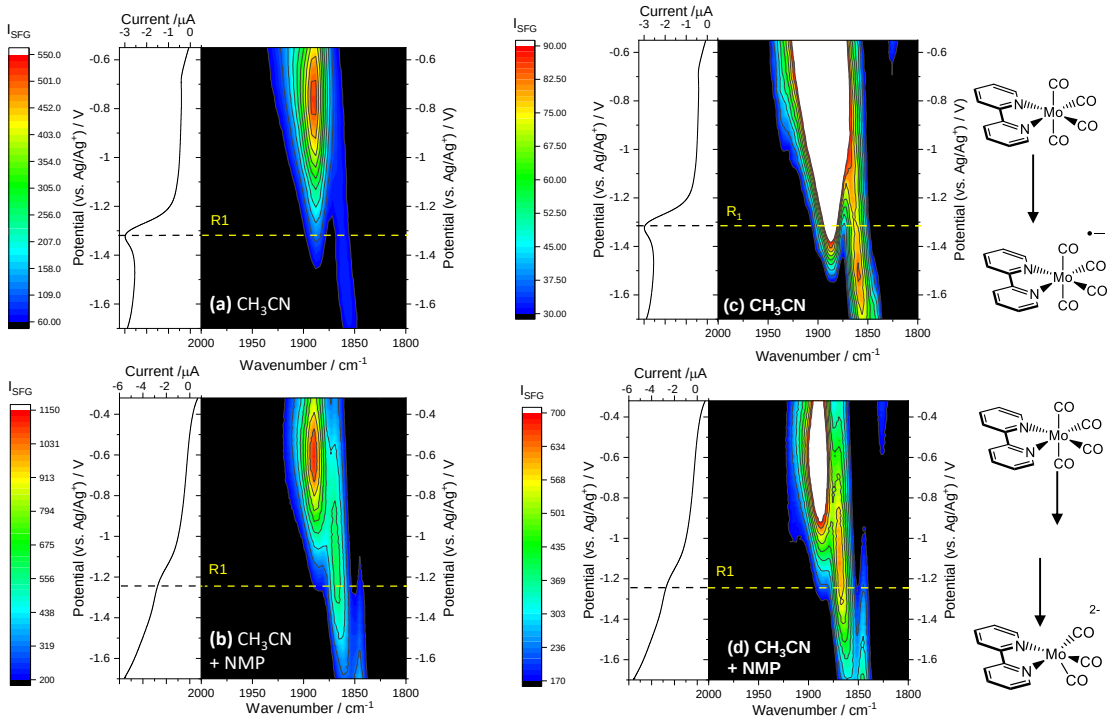

Figure 2. *VSFG spectra in the ν(CO) region of Mo(bpy)(CO)$_4$ (1 mM) in CH$_3$CN (a,c) and CH$_3$CN with 10% (vol.) NMP (b,d) during a linear sweep (5 mV s^{-1}, CH$_3$CN (a,c) and 2.5 mV s^{-1} 10% (vol.) NMP (b,d) positive to negative direction) with 0.1 M TBAPF$_6$ at a Au electrode under Ar, ppp polarisation. Parts (c,d) are replotted over a limited SFG intensity range. The chemical structures on the right-hand side represent the dominant species to which the VSFG spectra are assigned.*

Figure 2 shows VSFG spectra for the same polycrystalline Au electrode in a solution of Mo(bpy)(CO)$_4$ in CH$_3$CN and CH$_3$CN with 10% NMP under Ar as the potential is swept from approximately the open circuit voltage to negative of reduction 1 'R1'; see supporting information (note 1) for experimental details. The assignment of the VSFG spectra of Mo(bpy)(CO)$_4$ in CH$_3$CN has been reported previously,[11] and is briefly covered here; see supporting information note 2 for full details. Initially at -0.55 V, the spectrum is dominated by a band at ~1890 cm^{-1} due to a υ(CO) mode of Mo(bpy)(CO)$_4$, with the complex accumulating as the electrode is made more negative, Figure 2a.[10,11] Between -0.65 and -1.15 V the 1890 cm^{-1} υ(CO) band of Mo(bpy)(CO)$_4$ shifts in frequency with applied potential (4.5 ± 0.7 cm^{-1} V^{-1}, figure 3) demonstrating that the complex is at, or near to the electrode surface (within the double layer structure).[12,13] Weaker bands at 1905 cm^{-1}, ~1830 cm^{-1} and a shoulder at ~1870 cm^{-1} are also present between -0.55 and -1.15 V, Figure S3. The band at 1905 cm^{-1} is due to a concentration of Au-CO (Figure S3) whilst the weak bands at ~1830 cm^{-1} and 1870 cm^{-1} are assigned to Mo(bpy)(CO)$_4$.[11]

At approximately -1.3 V, reduction of Mo(bpy)(CO)$_4$ occurs (R1, figure 1, 2). The band at ~ 1890 cm^{-1} decreases and a new band at 1863 cm^{-1} grows in (tuning rate 19.3 ± 1.8 cm^{-1} V^{-1}, figure 3) assigned to the reduced species, Mo(bpy)(CO)$_4$$^{\bullet-}$.[10,11]At -1.5 V, when the VSFG spectra are replotted over a limited I_{VSFG} range (figure 2c) a weak band assignable to Mo(bpy)(CO)$_3^{2-}$ is detected (~1841 cm^{-1}). This is due to a small population of Mo(bpy)(CO)$_4^-$ undergoing CO loss and subsequent reduction at the Au electrode surface.[11]

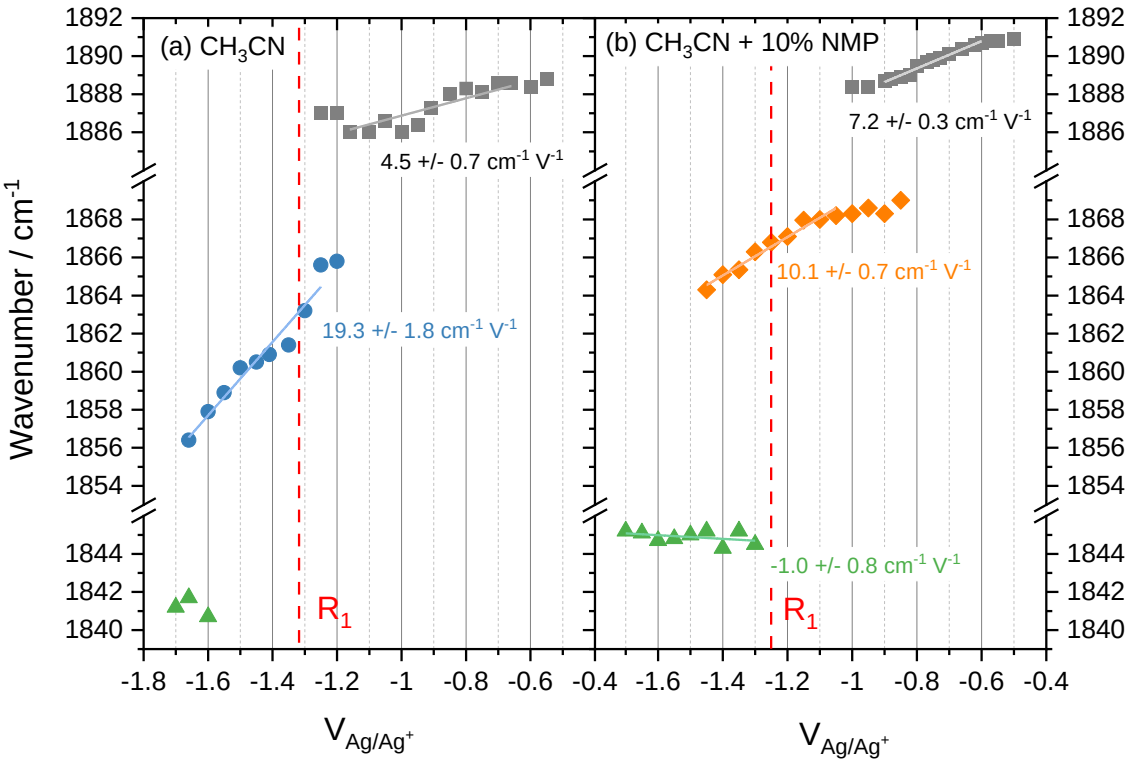

Figure 3. *Potential dependent ν(CO) frequencies during VSFG experiments of $Mo(bpy)(CO)_4$ in CH_3CN (a) and with 10% NMP (b). Grey squares assigned to $Mo(bpy)(CO)_4$, blue circles $Mo(bpy)(CO)_4^-$, green triangles $Mo(bpy)(CO)_3^{2-}$. We demonstrate below the orange diamonds in (b) is due to reoriented $Mo(bpy)(CO)_4$. The span of the fit lines indicates the potential range used to generate the tuning rate.*

When NMP is present, positive of -0.6 V the VSFG spectra (figure 2b) are similar to those recorded in CH_3CN alone, with a dominant band at ~1890 cm^{-1} and weaker bands at *ca.* 1830 and 1870 cm^{-1}, assignable to υ(CO) modes of $Mo(bpy)(CO)_4$. We conclude that the orientation and nature of interaction between the $Mo(bpy)(CO)_4$ and the Au surface positive of -0.6 V are similar in both the presence and absence of NMP.

Negative of -0.6 V, the VSFG spectra in the presence of NMP are markedly different. The ~1890 cm^{-1} $Mo(bpy)(CO)_4$ VSFG band decreases and a band at ~1870 cm^{-1} (-0.85 V, 10.1 ± 0.7 cm^{-1} V^{-1}) grows in, becoming dominant by -1.0 V. The decrease in intensity at ~1890 cm^{-1} does not correlate with a measured change in current *in-situ*. Separate CV and square wave voltammetry (SWV, figure 4) measurements also do not show any clear features in the potential window of interest (-0.6 to -1.0 V) assignable to Faradaic processes. We performed differential capacitance measurements of CH_3CN and CH_3CN + 10% NMP, figure 4c. These use a low concentration of $TBAPF_6$ (0.1 mM) to enable observation of the point of zero charge (pzc) and potentials where specific ion/solvent absorption occurs[14] in the absence of $Mo(bpy)(CO)_4$. The potential at pzc is approximately ~ 0.6 V for both solvent compositions, but the capacitance is different at potentials positive of pzc. With NMP we observe a broadening and shift to -0.6 V in the capacitance peak ,coinciding with the potential where there is an abrupt change in spectral activity (Figure 2). This indicates a potential dependent change in the double layer structure owing to the presence a small amount (10 % vol.) NMP.

With no Faradaic processes to explain the loss in VSFG intensity when NMP is present, we conclude that the change in the VSFG spectra is due to re-orientation of $Mo(bpy)(CO)_4$ at the electrode surface between -0.6 and -1.0 V as a result of the potential and solvent dependent double layer restructuring. The intensity of VSFG modes is dependent upon their relative orientation and we assign a reorientation of $Mo(bpy)(CO)_4$ as the cause of the decrease in the relative intensity of the ~1890 cm^{-1} band and increase in intensity of the 1870 cm^{-1} band. Supporting this assignment is the observation that the 1870 cm^{-1} band persists until R1 (-1.25 V, figure 2b) and that during CVs (-0.3 to -1.7 to -0.3 V, figure S2) the 1870 cm^{-1} band reforms at potentials slightly positive of O1 (-1.2 V, figure 1a). Reorientation of interfacial species as a result of changing field[15] and non-Faradaic potential dependent reactions[16] has been previously reported. Owing to the agreement in potential of R_1 in the presence and absence of NMP (Figure 1), and the abrupt change in spectral activity in the vicinity R_1 (Figure 2), we exclude the possibility that we observe a non-Faradaic transient product prior to R_1 in the presence of NMP in this work.

In the presence of NMP at potentials negative of R1 (-1.25 V) a new band at 1845 cm^{-1} grows as the band at 1870 cm^{-1} of $Mo(bpy)(CO)_4$ decays, figure 2. Through correlation of its appearance at potentials where catalysis onsets in NMP (figure 1) and through spectroelectrochemical studies,[10,11] we assign the band at 1845 cm^{-1} to $Mo(bpy)(CO)_3^{2-}$. By -1.6 V $Mo(bpy)(CO)_3^{2-}$, the active CO_2 reduction catalyst, is the dominant species at the electrode when NMP is present. In contrast in CH_3CN at -1.6 V $Mo(bpy)(CO)_4^-$ is dominant and the catalytic current is significantly lower.

We propose that in the presence of NMP, reorientation of $Mo(bpy)(CO)_4$ facilitates rapid (likely sub-second) CO loss from the initially formed $Mo(bpy)(CO)_4^-$ leading to $Mo(bpy)(CO)_3^-$ which is immediately reduced to $Mo(bpy)(CO)_3^{2-}$, consistent with the irreversibility of the R_1/O_1 redox couple in CV's at < 100 mV s^{-1}, Figure 4(a). The reduction potential of $Mo(bpy)(CO)_3^-$ has not been determined experimentally but DFT calculations, albeit without explicit solvent or the presence of the electrode and local electric field, show that $Mo(bpy)(CO)_3^-$ reduction occurs at potentials positive of $Mo(bpy)(CO)_4^-$,[17] supporting the proposed mechanism. It is known that photochemical ligand substitution of this class of complexes occurs at the axial sites[18] and it can be hypothesised that CO loss is facilitated from the tetracarbonyl by reorientation to make the axial CO groups accessible by making them parallel to the Au surface to enable interaction between the carbon atom and the electrode. In CH_3CN alone we observe only a slight change in the relative I_{VSFG} of the $Mo(bpy)(CO)_4$ bands as the potential is changed (figure S4) indicating that the applied potential is having less effect on the complex (see note S2) and the lack of reorientation hinders CO loss from $Mo(bpy)(CO)_4^-$.

In conclusion, the large increase in electrocatalytic activity of $Mo(bpy)(CO)_4$ when a small (10 % vol) amount of NMP is added to an electrolyte solution is shown to be due to a potential dependent solvent restructuring of the double layer that leads to reorientation of $Mo(bpy)(CO)_4$ at the electrode surface. This pre-activates the complex and leads to a greater yield, at less negative potentials of the active catalyst for CO_2 reduction ($Mo(bpy)(CO)_3^{2-}$). Determining the actual orientation of the complex by simulation is beyond state-of-the-art computational methodologies. This would require development of highly complex models of the double layer under potentiostatic control that includes explicit solvent, electrolyte ions and catalyst interactions on the complicated polycrystalline charged Au surface. The experiments reported here, and previously,[11] show that the geometry and structure of the molecular catalyst is dependent on all of these interactions, highlighting the complex nature of such studies. Until such in-silico models can be realised in-situ spectroscopic studies that specifically target the electrode interface remain vital for rationalising electrocatalytic activity.

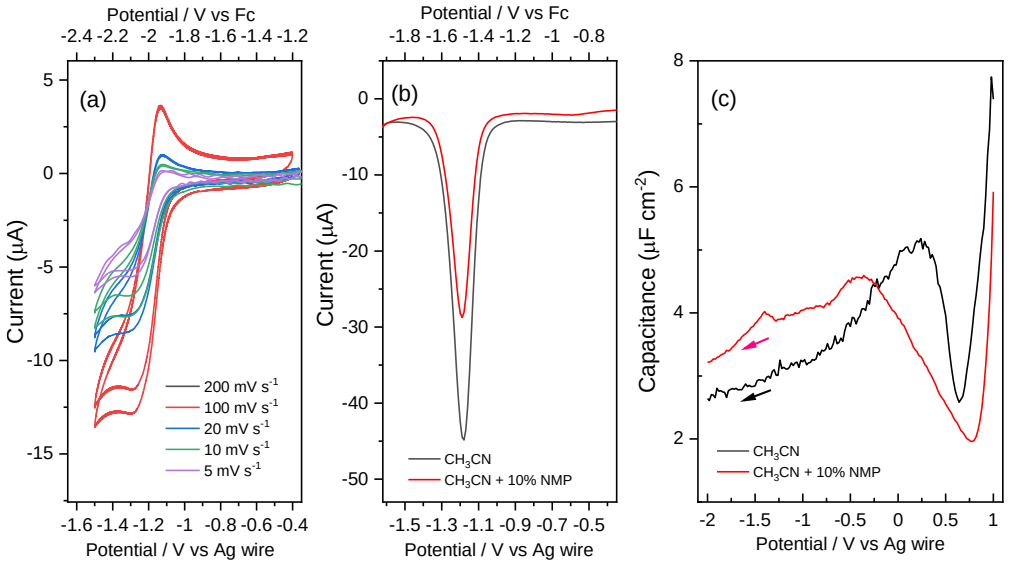

Figure 4. *Variable scan rate CV of R1 of Mo(bpy)(CO)$_4$ in CH$_3$CN with 10% NMP (b) SWV of R1 at 100 mV s^{-1}. Both (a) and (b) use 100 mM TBAPF$_6$. (c) Differential capacitance of the Au electrode in the presence and absence of NMP with 0.1 mM TBAPF$_6$ recorded at 10 Hz +1 V to -2 V vs Ag.*

Supporting information for publication: Experimental Details; Detailed discussion of spectral assignments.

Acknowledgements

This work was funded by UKRI-EPSRC (EP/P034497/1 and EP/S017623/1). VSFG measurements were performed at the University of Liverpool Early Career Laser Laboratory which is maintained and operated as a shared research facility by the Faculty of Science and Engineering. Initial experiments were carried out at the UK Central Laser Facility using ULTRA during experiment 16230052. We thank to Dr Gilberto Teobaldi (STFC Scientific Computing Department) and also Adam Piatt (University of Liverpool) for helpful discussions.

References

1. Kinzel, N. W.; Werle, C.; Leitner, W, Transition Metal Complexes as Catalysts for the Electroconversion of CO2: An Organometallic Perspective, *Angew. Chem., Int. Ed. Engl.* **2021**, 60 (21), 11628−11686. DOI:10.1002/anie.202006988

2. Taylor, J. O.; Leavey, R. D.; Hartl F., Solvent and Ligand Substitution Effects on the Electrocatalytic Reduction of CO_2 with [Mo(CO)$_4$(*x*,*x*′-dimethyl-2,2′-bipyridine)] (*x*=4-6) Enhanced at a Gold Cathodic Surface, *ChemElectroChem*, 2018, 5 (21), 3155–3161**.** DOI:10.1002/celc.201800879

3. Clark, M. L.; Grice, K. A.; Moore, C. E.; Rheingold, A. L.; Kubiak, C. P.; Electrocatalytic CO2 reduction by M(bpy-R)(CO)$_4$ (M = Mo, W; R = H, tBu) complexes. Electrochemical, spectroscopic, and computational studies and comparison with group 7 catalysts, *Chem. Sci*., **2014**, 5, 1894. DOI:10.1039/C3SC53470G

4. Ringe, S.; Clark, E. L.; Resasco, J.; Walton, A.; Seger, B.; Bell, A. T.; Chan, K Understanding cation effects in electrochemical CO2 reduction, Energy Environ. Sci., **2019**, 12, 3001–3014 DOI:10.1039/C9EE01341E

5. Resasco, J.; Chen, L. D.; Clark, E.; Tsai, C.; Hahn, C.; Jaramillo, T. F.; Chan, K.; Bell, A. T.; Promoter Effects of Alkali Metal Cations on the Electrochemical Reduction of Carbon Dioxide, *J. Am. Chem. Soc.*, **2017**, 139, 11277–11287. DOI:10.1021/jacs.7b06765

6. Yu, J.; Yin, J.; Li, R. Ma, Y; Fan, Z.; Interfacial electric field effect on electrochemical carbon dioxide reduction reaction, **2022**, 2 (9), 2229-2252 DOI:10.1016/j.checat.2022.07.024

7. Kaminsky, C. J.; Weng, S.; Wright, J.; Surendranath Y.; Adsorbed cobalt porphyrins act like metal surfaces in electrocatalysis, *Nature Catalysis*, **2022**, 5, 430-442. DOI:10.1038/s41929-022-00791-6

8. Fried, S. D.; Bagchi, S.; Boxer, S. G.; Extreme electric fields power catalysis in the active site of ketosteroid isomerase. *Science*, **2014**, 346, 1510–1514. DOI:10.1126/science.1259802

9. Bullock, R. M.; Chen, J. G.; Gagliardi, L.; Chirik, p. J.; Farha, O. K.; Hendon, C. H.; Jones, C. W.; Keith, J. A.; Klosin, J.; Minteer, S. D.; Morris, R. H.; Radosevich, A. T.; Rauchfuss, T. B.; Strotman, N. A.; Vojvodic, A.; Ward, T. R.; Yang, J. Y.; Surendranath Y.; Using nature's blueprint to expand catalysis with Earth-abundant metals, *Science*, **2020**, 369, eabc3183. DOI:10.1126/science.abc3183

10. Tory, J.; Setterfield-Price, B; Dryfe, R. A. W; Hartl, F, [M(CO)4(2,2'-bipyridine)] (M=Cr, Mo, W) Complexes as Efficient Catalysts for Electrochemical Reduction of CO2 at a Gold Electrode, *ChemElectroChem*, **2015**, 2, 213 – 217. DOI: 10.1002/celc.201402282

11. Neri, G; Donaldson, P. M; Cowan, A. J., The Role of Electrode–Catalyst Interactions in Enabling Efficient CO_2 Reduction with Mo(bpy)$(CO)_4$ As Revealed by Vibrational Sum-Frequency Generation Spectroscopy, *J. Am. Chem. Soc.*, **2017**, 139, 13791−1379. DOI: 10.1021/jacs.7b06898

12. Bishop, D. M.; Vibrational Stark Effect, *Journal Chem. Phys.*, **1993**, 98, 3179–3184. DOI:10.1063/1.464090

13. Rey, N.G.; Dlott, D. D.; Studies of electrochemical interfaces by broadband sum frequency generation, *J. Electroanal. Chem.*, **2017**, 800, 114–125. DOI:10.1016/j.jelechem.2016.12.023

14. Shatla, A. S.; Landstorfer, M.; Baltruschat, H.; On the Differential Capacitance and Potential of Zero Charge of Au(111) in Some Aprotic Solvents *ChemElectroChem*, **2021**, 8, 1817-1835. DOI:10.1002/celc.202100316

15. Sampaio, R. N., Li, G., Meyer, G. J., Flipping molecules over on TiO2 surfaces with light and electric fields, *J. Am. Chem. Soc.*, **2019**, 141, 13898-13904. DOI: 10.1021/jacs.9b06687

16. Sarkar, S. Maitra, A., Lake, W. R., Warburton, R. E., Hammes-Schiffer S., Dawlaty, J. M.; Mechanistic Insights about Electrochemical Proton-Coupled Electron Transfer Derived from a Vibrational Probe, *J. Am. Chem. Soc.*, **2021**, 143, 8381-8390. DOI: 10.1021/jacs.1c01977.

17. Isegawa, M., Group 6 (Cr, Mo, W) and Group 7 (Mn, Re) bipyridyl tetracarbonyl complex for electrochemical CO2 conversion: DFT and DLPNO-CCSD(T) study for effects of the central metal on redox potential, thermodynamics, and kinetics, *Chemical Physics*, **2023**, 565, 111758.

18. Miholová, D.; Vlček A. A.; ELECTRODE-CATALYZED SUBSTITUTION OF M$(CO)_4$bipy (M = Cr, MO, W) INITIATED BY REDUCTION, *Journal of Organometallic Chemistry*, **1985**, 279, 317-326.

TOC Figure